VLA observations of the "water fountain" IRAS 16552−3050

Olga Suárez[1,2], José F. Gómez[2], Luis F. Miranda[2]

ABSTRACT

We present Very Large Array (VLA) observations of the water maser emission towards IRAS 16552-3050. The maser emission shows a velocity spread of $\simeq$ 170 km s^{-1}, and a bipolar distribution with a separation between the red and blueshifted groups of $\simeq 0.08''$. These observations and the likely post-AGB nature of the source indicate that IRAS 16552-3050 can be considered as a member of the "water fountain" class of sources (evolved stars showing H_2O maser emission with a velocity spread $\gtrsim$ 100 km s^{-1}, probably tracing collimated jets). The water maser emission in IRAS 16552-3050 does not seem to be associated with with any known optical counterpart. Moreover, this source does not have a near-IR 2MASS counterpart, as it happens in about half of the water fountains known. This suggests that these sources tend to be heavily obscured objects, probably with massive precursors ($\gtrsim 4-5$ M$_\odot$). We suggest that the water maser emission in IRAS 16552-3050 could be tracing a rapidly precessing bipolar jet.

Subject headings: masers – stars: AGB and post-AGB – stars: individual (IRAS 16552−3050) – stars: mass loss – stars: winds, outflows

1. Introduction

Water fountains are evolved Asymptotic Giant Branch (AGB) and young post-AGB stars that show water maser emission with velocity separations in their spectral features $\geq$100 km s^{-1} (Likkel & Morris 1988). Some of them have been observed with radio interferometric techniques and all show bipolar distributions of their H_2O maser emission, indicating the presence of jets with extremely short dynamical ages of 5-100 yr (Likkel & Morris 1988; Boboltz & Marvel 2005, 2007; Imai et al. 2002, 2004; Imai 2007). OH maser emission has been detected in most sources catalogued as water fountains and, in general, this emission

[1]UMR 6525 H.Fizeau, Univ. Nice Sophia Antipolis, CNRS, OCA. Parc Valrose, F-06108 Nice cedex 02, France. olga.suarez@unice.fr

[2]Instituto de Astrofísica de Andalucía, CSIC, Apartado 3004, E-18080 Granada, Spain

exhibits lower velocities and is spatially less extended than that of H_2O (see, for example Deacon et al. 2007). Water fountains are evolutionarily located between two phases of stellar evolution, AGB stars and planetary nebulae (PNe), when mass-loss properties, among others, change dramatically. While mass ejection during the AGB phase is spherical, most PNe exhibit elliptical, bipolar, or multipolar morphologies. These morphologies have been attributed to the action of collimated outflows on the previously expelled spherical AGB shell (Sahai & Trauger 1998). Therefore, water fountains very probably trace the onset of non-spherical and highly collimated mass ejection. Understanding the transformation of an AGB star into a PN relies on a precise knowledge of the properties and evolution of water fountains. Unfortunately, very few water fountains are known at present (11 sources reported as of March 2008, see Imai 2007), so that adding new members to this important class of objects represents a valuable progress.

Recently, in a single-dish search for H_2O masers in evolved stars, Suárez et al. (2007) found water maser emission toward IRAS 16552−3050 (hereafter IRAS16552), with a maximum separation among its velocity components of ∼170 km s^{-1}. IRAS16552 was first proposed to be a candidate post-AGB star by Preite-Martinez (1988), based on its IRAS colors. A possible optical counterpart of the IRAS far-infrared source was classified by Hu et al. (1993) and Suárez et al. (2006) as a star of spectral type K9III and K0I, respectively.

In this paper, we present Very Large Array (VLA) observations, carried out to confirm the association of this high-velocity water maser emission with the IRAS source, and to determine the spatial distribution of the masers. Our results allow us to include IRAS16552 as a bona fide member of the water fountain class. In Sec. 2 we describe the performed observations. Sec. 3 presents the obtained results, and Sec. 4 a discussion on the properties of IRAS16552 and a comparison of this source with other water fountains. Finally, in Sec. 5 we summarize the main conclusions of this work.

2. Observations and data reduction

We have observed the $6_{16} - 5_{23}$ maser transition of the water molecule (rest frequency = 22235.08 MHz) using the VLA of the National Radio Astronomy Observatory (NRAO)[1] in two separate epochs. In the first one (2006 March 22 and 26), we used the A configuration of the VLA, and observed the right circular polarization (1 IF mode) over a bandwidth of 3.11 MHz sampled with 255 channels (thus providing a spectral resolution of 1.22 kHz, or

[1]The National Radio Astronomy Observatory is a facility of the National Science Foundation operated under cooperative agreement by Associated Universities, Inc.

0.16 km s^{-1}). To be able to cover the whole range of the water maser emission detected by Suárez et al. (2007) toward IRAS16552, we successively centered the bandwidth at six different velocities with respect to the Local Standard of Rest (LSR): −70, −30, and +10 km s^{-1} on 2006 March 22, and +50, +85, and +120 km s^{-1} on 2006 March 26. Therefore, we covered the water maser emission of IRAS16552 on a velocity range from −91 to +141 km s^{-1} (although not simultaneously). The phase center for these observations was set at R.A.(J2000) = $16^h58^m27.84^s$, Dec.(J2000) = $-30°55'06.7''$, which is within $1''$ from the position of the source given in Suárez et al. (2006).

In the second epoch, carried out on 2007 December 24, we used the B configuration of the VLA and the 4 IF mode, with a bandwidth of 3.08 MHz sampled with 63 channels for each IF (48.83 kHz, or 0.7 km s^{-1} spectral resolution). Two IFs were used to observe right and left circular polarizations (RCP and LCP) centering the bandwidth at $v_{\rm LSR} = -60$ km s^{-1}, while the other two IFs (RCP and LCP) were centered at $v_{\rm LSR} = +89.6$ km s^{-1}. Based on the results of the first epoch, we set the phase center of these observations at R.A.(J2000) = $16^h58^m27.3^s$, Dec.(J2000) = $-30°55'08''$, to include all observed maser components within $1''$ from this center.

For both epochs, source J1331+305 was used as the flux calibrator (assumed flux density $\simeq 2.54$ Jy), J1229+090 was the bandpass calibrator (bootstrapped flux density $\simeq 20.5 \pm 1.1$, 26.4 ± 0.4, and 25.2 ± 0.4 Jy on 2006 March 22, 2006 March 26, and 2007 December 24, respectively) , while J1626-298 was the phase calibrator (bootstrapped flux density $\simeq 1.00 \pm 0.09$, 1.72 ± 0.03, and 2.30 ± 0.04 Jy on 2006 March 22, 2006 March 26, and 2007 December 24, respectively). Maps were obtained with robust weighting of visibilities (Robust parameter = 0) and deconvolved using the CLEAN algorithm. The resulting synthesized beams were $\simeq 0.20'' \times 0.07''$ and $\simeq 0.7'' \times 0.25''$ for the first (A configuration) and second (B configuration) epochs, respectively, with their major axes oriented nearly north-south.

Data were self-calibrated using a strong maser feature, and applying the obtained phase and amplitude correction to the rest of the channels for each data set. In the first epoch, the maser components detected in each day (2006 March 22 and 26, i.e., blue and redshifted emission, respectively) could be aligned to a common reference position, using spectral features that were present in the overlapping region between each individual observation. However, the data taken in different days could not be aligned since there was no common spectral feature in the velocity ranges covered. Therefore, the 2σ relative positional uncertainty between the maser features observed on the same day in the first epoch is $\lesssim 0.001''$ (estimated as $2\sigma \simeq \frac{\Delta\theta}{\rm SNR}$, where $\Delta\theta$ is the size of the primary beam and SNR is the signal to noise ratio), while the positional uncertainty among the emission observed in different days is $\simeq 0.1''$. For the second epoch, since all data were taken simultaneously, the self-calibration corrections

obtained for the strongest maser feature was applied to all channels. The relative positional accuracy among all features in that second epoch was $\lesssim 0.005''$

3. Results

The spectrum and the spatial distribution of the water maser components obtained on the first epoch are shown in Fig. 1. By "maser components" we mean individual intensity peaks in the spectrum. The positional information has been obtained by fitting elliptical gaussians to the maser emission, only in the channels in which a spectral peak is present. The total velocity span of the maser emission is $\simeq$170 km s^{-1}. Two groups of components are evident in the spectrum: the redshifted group, from 50 to 110 km s^{-1}, and the blueshifted one, from -40 to -80 km s^{-1}. The red components are more numerous and more intense than the blue ones, with the most intense peak reaching $\simeq$ 5.1 Jy. The two groups appear spatially separated by $\simeq 0.11''$, forming a bipolar distribution, with the red components clustered at the NE and the blue components clustered at the SW. However, as explained in Sec. 2, while the spatial distribution of components within either group is very reliable (relative positional errors $\leq 0.001''$), the relative position between both groups has an error of $\simeq 0.1''$ (since they were observed in different days), which is on the order of the apparent separation. Therefore, the bipolar distribution of the maser emission observed in the first epoch may not have been real.

Fig. 2 shows the spectrum and the spatial distribution of the water maser emission obtained in the second epoch. These observations did not cover the whole velocity range in which emission is present. They were set up to simultaneously observe red- and blueshifted components, in order to confirm the bipolarity. In these data, the NE-SW bipolar distribution is present, with a separation of $\simeq 0.08''$ between the centroids of the red and blue groups along position angle (PA) $\simeq 44^{\rm o}$. The separation and PA are both more reliable for this second epoch (relative position error between features $\simeq 0.005''$), although the internal distribution of the components in either group is more accurate in the first epoch. Therefore, water maser emission from IRAS16552 seems to trace a bipolar outflow with a projected size of $\simeq 0.08''$, and velocity along the line of sight of $\simeq$ 85 km s^{-1} (half of the total velocity span). Our results confirm IRAS16552 as a water fountain with a bipolar distribution of its water maser emission. It also confirms the trend of bipolarity in all water fountains studied up to now at high angular resolution with radio interferometry, strongly suggesting that water masers in all water fountains are produced in collimated, bipolar jets.

The centroid position of the individual water maser components has absolute coordinates R.A.(J2000) = $16^h58^m27.30^s$, Dec(J2000) = $-30°55'8.0''$ (absolute position error $\simeq 0.1''$,

compatible in both epochs). Assuming a bipolar configuration for the jet, we expect the powering source to be located near that position. However, this centroid is $\simeq 16''$ away from the post-AGB star identified at optical wavelengths by Suárez et al. (2006), indicating that the water maser emission is associated with a different evolved star within the field. Note that there is an error in the possition given in Table 3 of Suárez et al. (2006), since this position does not correspond to the K0I star marked in the identification chart and whose spectrum is shown in that paper, but to a nearby source (2MASS J16582776-3055062). The true coordinates for the K0I star identified in Suárez et al. (2006) are R.A.(J2000) = $16^h58^m28.53^s$, Dec(J2000) = $-30^\circ55'09.3''$.

We have searched the DSS plates and the 2MASS catalog for an optical and/or near IR counterpart at the position of the outflow source, but although several optical and near-IR sources lie within the IRAS ellipse error, none of them is coincident with the position of the maser emission. The closest 2MASS source, J16582725-3055108, does not coincide within the errors ($0.5''$ for 2MASS) with the maser position, since it is located at $2.3''$ from the centroid position. This implies that the outflow source must be heavily obscured by its circumstellar envelope. From these results, it is plausible that the IRAS point source actually traces this obscured source that is powering the masers, but it is not related to the optical source. In this case, the IRAS colors will classify IRAS16552 as a post-AGB star, a classification also supported by its low IRAS variability. Its likely post-AGB nature, together with its association with high-velocity bipolar water-maser emission further indicates that IRAS16552 belongs to the water fountain class.

As for the spatial distribution of water masers within each group, the redshifted (NE) cluster of masers is oriented almost along the north-south direction and extends $\simeq 0.04''$-$0.05''$ in both epochs. The SW group is also oriented almost north-south in the first epoch and extends $\simeq 0.03''$. The distribution in the second epoch looks somewhat different, with an orientation along PA $\sim 45^\circ$, but given the relative errors (see Sec. 2), the distribution in this second epoch is less reliable. In any case, it seems clear that, if we assume that the line joining the red- and blueshifted groups traces the jet direction, the maser emission within each group is not elongated along this jet.

As shown in Figs. 1 and 2, the maser components within the redshifted cluster tend to be grouped according to their velocities, although the apparent grouping seems to be different in the two epochs. In the first epoch, the least redshifted group, with $v \leq 60$ km s^{-1} is located at the north, almost all the components of the intermediate-velocity group ($60 \leq v \leq 80$ km s^{-1}) are located at the south, and the most redshifted components ($v \geq 80$ km s^{-1}) are situated in between the other two groups. In the second epoch, the group centered $\simeq 75$ km s^{-1} is north of the one centered $\simeq 90$ km s^{-1}, which is the opposite distribution to the one in the

first epoch. We note again that in the second epoch we did not observe the same velocity range as in the first one, and the positional error among the components of each group is larger in the second one ($\simeq 0.005''$ as compared to $\simeq 0.001''$). In the SW group, no clear tendency in the distribution of radial velocities is seen in either epoch.

4. Discussion

4.1. A comparison of IRAS16552 with other water fountains

The absence of near IR counterpart in the Two Micron All Sky Survey (2MASS) catalog (Skrutskie et al. 2006) does not seem to be an uncommon characteristic in the water fountains. Of the 11 water fountains reported so far (those listed in Imai 2007) all those covered by the Midcourse Space Experiment (MSX) catalog (Egan et al. 2003) (only IRAS16552 was not included in the MSX survey) have a mid-infrared counterpart. However, we have found 2MASS counterparts (coincident with MSX sources within the errors) for only 5 of them. We did not find any significant relationship between the presence of a near IR counterpart and the characteristics of the water masers, such as number of maser components, dynamical age, or velocity span. The still small number of water fountains known is an obvious hindrance for this type of comparison. However, the fact that about half of the water fountains are not detected in the near IR gives us hints about the characteristics of their envelopes compared to those of the rest of AGB and post-AGB stars. Both AGB and post-AGB stars are usually detected in the near IR, although a large fraction of AGB stars, and some post-AGB stars are not detected in the optical (Suárez et al. 2006). This suggest that the central stars of water fountains are surrounded by thicker envelopes than in the rest of AGB and post-AGB stars. This could be explained if the evolution into the post-AGB stage is faster in water fountain sources, and therefore, these stars are relatively massive ($\gtrsim 4-5$ M$_\odot$). Nevertheless, a study of the near IR properties of water fountains, with a higher sensitivity than the data in the 2MASS catalog may yield the detection of weak counterparts, provided that an accurate position of the water maser emission is determined with radio interferometric observations.

In order to place IRAS16552 in the evolutionary framework of water fountains, we have plotted all such sources known on an IRAS two-color diagram (Fig. 3), where we also show their dynamical ages (for those known). It is interesting that water fountains tend to be distributed in this IRAS color-color diagram on the same region as post-AGB stars (Suárez et al. 2006), while in this region, few AGB stars are located (Jiménez-Esteban et al. 2006). This is certainly reasonable, given that water fountains seem to be post-AGB or evolved AGB stars. However, it is potentially important, since it suggests that IRAS colors could be useful as diagnostics to select potential candidate sources in future searches for

water fountains among the most extreme AGB stars.

To try to establish the evolutionary stage for each of the water fountains we have used the [8]−[12] *vs* [15]−[21] MSX two-color diagram (see Fig 4). Sevenster (2002) has studied the position of OH-maser-emitting AGB and post-AGB sources in this diagram. The diagram has been divided in four quadrants (QI, QII, QIII, QIV), with classical AGB stars located in QIII (low left), early post-AGB stars in the QIV (low right) and more evolved objects in the QI, while QII contains star forming regions. The two water fountains with the shortest dynamical age are located in region III, and the one with the longest in region I, which agrees with Sevenster's evolutionary distribution. Estimates of the dynamical ages of the rest of water fountains will be helpful to confirm this trend. Moreover, the objects with visible lobes (IRAS 16342−3814 and IRAS 19134+2131) are in the QIV and QII region, always with [8]−[12]>0.9. According to Sevenster (2002), the transition from [8]−[12]<0.9 to [8]−[12]>0.9 implies the transition from AGB to post-AGB stars.

The water maser components in water fountains seem to show always a spatial bipolar layout, although their distribution is rather different from one object to another. Also the number of components is very variable from one source to another. There are sources as OH12.8−0.9 which show only 2 or 3 water maser components with very similar velocities at the tips of each lobe (Boboltz & Marvel 2005, 2007), and sources as IRAS 18286−0959 that show multiple components with significant velocity dispersion within each lobe, and also components located close to the center of the maser distribution, with intermediate velocities between those of the most extreme components (Imai 2007). In the case of IRAS16552, it shows at least 15 components with a spread in velocities within each lobe of $\simeq 25 - 50$ km s^{-1}, and an absence of equatorial masers. These spectral and spatial characteristics make it similar to other water fountains as IRAS 16342−3814 (Morris et al. 2003), or IRAS 19134+2131 (Imai et al. 2004, 2007).

We note that single-dish observations of the OH maser line at 1612 MHz did not show any maser emission in IRAS16552 (Te Lintel Hekkert et al. 1991; Hu et al. 1994), with 1σ rms of 0.2, and 0.1 Jy, respectively. The presence or not of OH maser emission, as well as its kinematical and spatial characteristics is of potential interest to further characterize water fountains. The presence of OH maser emission is a common characteristic in almost all water fountains. Apart from IRAS16552, the only other known water fountain in which OH seems not to be present is IRAS 19134+2131 (Lewis et al. 1987; Hu et al. 1994). The OH masers detected are in general less extended and have a smaller range of velocities than the H_2O masers, as is the case of IRAS 18043−2126 (Sevenster & Chapman 2001; Deacon et al. 2007), OH12.8−0.9 (Boboltz & Marvel 2005), W43A (Imai et al. 2002). This suggest that the OH masers tend to trace the former AGB shell, rather than the later bipolar mass-loss

traced by H_2O. However, the cases of IRAS 15445-5449 and IRAS 15544-5332 (Deacon et al. 2004, 2007) do not follow this trend, since OH maser emission in these sources have been found outside the velocity range of the H_2O masers. IRAS 16342−3814 can be considered as another exception since although the OH masers have a smaller velocity range than the H_2O masers (70 km s^{-1} vs 160 km s^{-1}; Sahai et al. 1999; Zijlstra et al. 2001; Likkel & Morris 1988; Morris et al. 2003), they are located in the bipolar jets and have a velocity that does not correspond to the AGB shell.

4.2. The orientation of the water maser distribution

As we mentioned in Sec. 3, the water maser emission in IRAS16552 is not aligned with the apparent jet direction. Such misalignment is also common in other sources, as IRAS 19134+2131 (Imai et al. 2004, 2007) and W43A (Imai et al. 2002). Those cases can be explained as the effect of ballistic corkscrew jets (Imai 2007; Vlemmings et al. 2006), where the masers are emitted in a ballistic way along the direction of a jet that precesses with time. This precession could be due to the presence of a binary stellar companion or a massive planet. These companions would also account for the magnetic fields found in sources as W43A (Vlemmings et al. 2006). Nevertheless, no direct evidence for a companion has been found so far in any water fountain.

IRAS16552 is an extreme case in which the water maser components are oriented almost perpendicular to the radial direction from the central source (assumed to be at the center of the distribution of the components, see Sec. 3). An almost perpendicular distribution is also seen in IRAS 16342−3814 (Morris et al. 2003) and OH 12.8-0.9 (Boboltz & Marvel 2005), which has been attributed to the masers tracing a shock front. For IRAS16552, such an interpretation would imply a rather large opening angle of the jet ($\simeq 70^\circ$). A possible alternative explanation is that the water masers in IRAS16552 trace a rapidly precessing/rotating bipolar jet. If the precession/rotation period is very short, as compared with the expansion timescale determined by the jet velocity, the bipolar jet (or the shocked regions in the neutral envelope) will describe point-symmetric structures oriented almost perpendicular to the outflow direction. At least qualitatively, this scenario may account for the observations of IRAS16552, specially for the first epoch, in which the distribution of masers within each group has been determined with a higher accuracy.

Remarkably, many PNe show collimated structures oriented almost perpendicular to the radial direction from the central star. This is the case of bipolar and elliptical PNe that exhibit a point-symmetric intensity distribution in the shell as, for instance, Hb5 (Corradi & Schwarz 1993) and Cn3-1 (Miranda et al. 1997). More interesting is the case of

components DD' in NGC6543 (Balick & Hajian 2004), which are dense (10^4 - 10^5 cm^{-3}) filaments that have been interpreted as due to a rapidly precessing bipolar jet (Miranda & Solf 1992). Given that water fountains are probably related to relatively massive stars (Sec. 4.1), their evolution through the post-AGB phase should be very fast. The fingerprints of rapidly precessing, collimated post-AGB outflows, such as the one proposed for IRAS16552, may still be present in the envelope when the central star ionizes the nebula and could show up as point-symmetric ionized filaments in PNe, similar to the components DD' in NGC6543.

5. Conclusions

In this paper we have presented VLA observations of H_2O masers at 22 GHz towards IRAS 16552−3050. Our main conclusions are as follow:

- We have found that the water maser emission in IRAS 16552−3050 span a velocity range of ∼170 km s^{-1} and shows a bipolar distribution of $\simeq 0.08$" in size. The properties of the water maser emission and the likely post-AGB nature of the central source allow us to confirm IRAS 16552−3050 as a member of the class of "water fountain" evolved objects.

- Our result confirms the trend of bipolarity in all water fountains known up to now, strongly suggesting that water masers in these sources are produced in bipolar, collimated jets.

- The water maser emission in IRAS 16552−3050 does not seem to be associated with the optical source identified by Hu et al. (1993) and Suárez et al. (2006), but with a different evolved object, for which there is no optical nor near-IR counterpart known.

- About half of the water fountains known do not have a near-IR counterpart in the 2MASS catalog. This suggest that water fountains are surrounded by thicker envelopes than the rest of AGB and post-AGB stars (which usually have near-IR counterparts), probably implying that they are relatively massive objects ($\gtrsim 4-5$ M$_\odot$).

- The distribution of the water maser emission in the red- and blueshifted group is almost perpendicular to the proposed jet direction. This might be explained if the maser emission traces a rapidly precessing/rotating bipolar jet. A later evolution could give rise to point-symmetric filaments observed in some PNe, which appear oriented almost perpendicular to the radial direction from the central star.

The authors with to thank Drs. G. Anglada and M. Osorio for useful discussions. JFG and LFM acknowledge support from Ministerio de Ciencia e Innovación (Spain), grants AYA 2005-08523-C03 and AYA 2005-01495, respectively, co-funded with FEDER funds. OS, JFG, and LFM are also supported by Consejería de Innovación, Ciencia y Empresa of Junta de Andalucía. This publication makes use of data products from the Two Micron All Sky Survey, which is a joint project of the University of Massachusetts and the Infrared Processing and Analysis Center/California Institute of Technology, funded by the National Aeronautics and Space Administration and the National Science Foundation.

REFERENCES

Balick, B. & Hajian, A. R. 2004, AJ, 127, 2269

Bedijn, P. J. 1987, A&A, 186, 136

Boboltz, D. A. & Marvel, K. B. 2005, ApJ, 627, L45

—. 2007, ApJ, 665, 680

Corradi, R. L. M. & Schwarz, H. E. 1993, A&A, 269, 462

Deacon, R. M., Chapman, J. M., & Green, A. J. 2004, ApJS, 155, 595

Deacon, R. M., Chapman, J. M., Green, A. J., & Sevenster, M. N. 2007, ApJ, 658, 1096

Egan, M. P., Price, S. D., Kraemer, K. E., Mizuno, D. R., Carey, S. J., Wright, C. O., Engelke, C. W., Cohen, M., & Gugliotti, M. G. 2003, VizieR Online Data Catalog, 5114, 0

Hu, J. Y., Slijkhuis, S., de Jong, T., & Jiang, B. W. 1993, A&AS, 100, 413

Hu, J. Y., Te Lintel Hekkert, P., Slijkhuis, F., Baas, F., Sahai, R., & Wood, P. R. 1994, A&AS, 103, 301

Imai, H. 2007, in IAU Symposium, Vol. 242, Astrophysical Masers and their Environments, ed. W. Baan & J. Chapman (Cambridge: Cambridge Univ. Press), 279

Imai, H., Morris, M., Sahai, R., Hachisuka, K., & Azzollini F., J. R. 2004, A&A, 420, 265

Imai, H., Obara, K., Diamond, P. J., Omodaka, T., & Sasao, T. 2002, Nature, 417, 829

Imai, H., Sahai, R., & Morris, M. 2007, ApJ, 669, 424

Jiménez-Esteban, F. M., García-Lario, P., Engels, D., & Perea Calderón, J. V. 2006, A&A, 446, 773

Lewis, B. M., Eder, J., & Terzian, Y. 1987, AJ, 94, 1025

Likkel, L. & Morris, M. 1988, ApJ, 329, 914

Miranda, L. F. & Solf, J. 1992, A&A, 260, 397

Miranda, L. F., Vazquez, R., Torrelles, J. M., Eiroa, C., & Lopez, J. A. 1997, MNRAS, 288, 777

Morris, M. R., Sahai, R., & Claussen, M. 2003, Rev. Mexicana Astron. Astrofis.Conf., 15, 20

Preite-Martinez, A. 1988, A&AS, 76, 317

Sahai, R., Te Lintel Hekkert, P., Morris, M., Zijlstra, A., & Likkel, L. 1999, ApJ, 514, L115

Sahai, R. & Trauger, J. T. 1998, AJ, 116, 1357

Sevenster, M. N. 2002, AJ, 123, 2772

Sevenster, M. N. & Chapman, J. M. 2001, ApJ, 546, L119

Skrutskie, M. F., Cutri, R. M., Stiening, R., Weinberg, M. D., Schneider, S., Carpenter, J. M., Beichman, C., Capps, R., et al. 2006, AJ, 131, 1163

Suárez, O., García-Lario, P., Manchado, A., Manteiga, M., Ulla, A., & Pottasch, S. R. 2006, A&A, 458, 173

Suárez, O., Gómez, J. F., & Morata, O. 2007, A&A, 467, 1085

Te Lintel Hekkert, P., Caswell, J. L., Habing, H. J., Haynes, R. F., Haynes, R. F., & Norris, R. P. 1991, A&AS, 90, 327

Vlemmings, W. H. T., Diamond, P. J., & Imai, H. 2006, Nature, 440, 58

Zijlstra, A. A., Chapman, J. M., te Lintel Hekkert, P., Likkel, L., Comeron, F., Norris, R. P., Molster, F. J., & Cohen, R. J. 2001, MNRAS, 322, 280

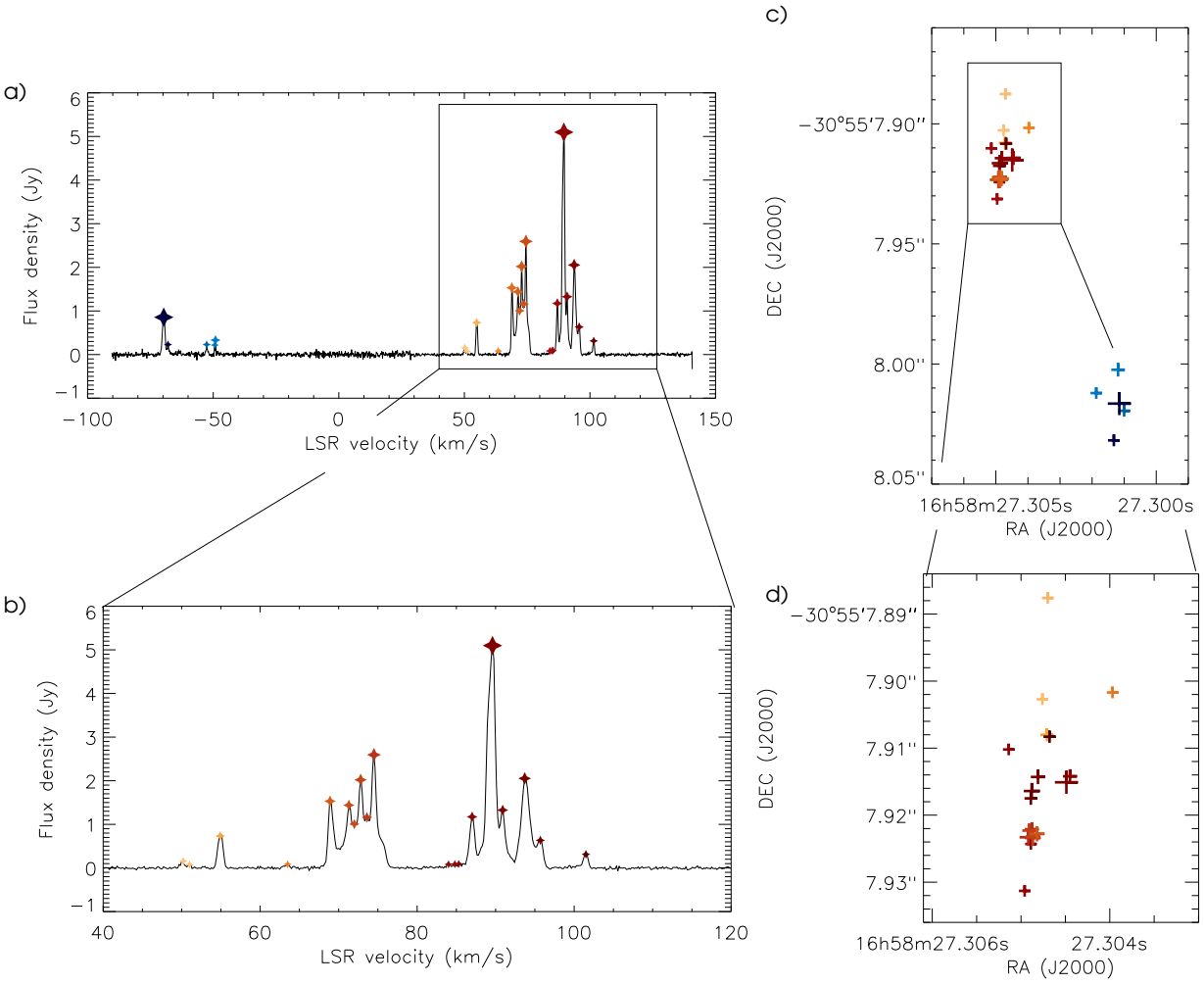

Fig. 1.— (a) Spectrum of the water masers towards IRAS 16552−3050, observed on 2006 March. The different maser components are identified by colored stars. The color code is used to identify the same components in the rest of the panels. (b) Close up of the redshifted part of the spectrum. (c) Spatial distribution of the peaks of the maser components. Note that the coordinates in the figure should be considered only as nominal. The error in absolute position is $\simeq$ 0.1" (see Sec. 2). (d) Close up of the spatial distribution, showing only the redshifted components. The symbol size increases with flux density.

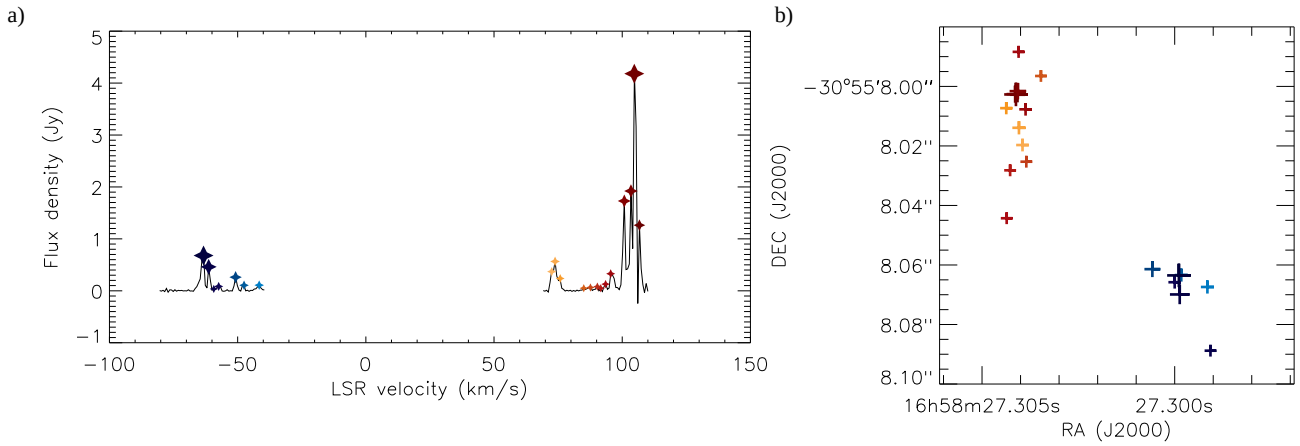

Fig. 2.— a) Spectrum of the water masers towards IRAS 16552−3050, observed on 2007 December. The different maser components are identified by colored stars. The color code is used to identify the same components in panel b. (b) Spatial distribution of the peaks of the maser components. Note that the coordinates in the figure should be considered only as nominal. The error in absolute position is $\simeq 0.1$" (see Sec. 2). The symbol size increases with flux density.

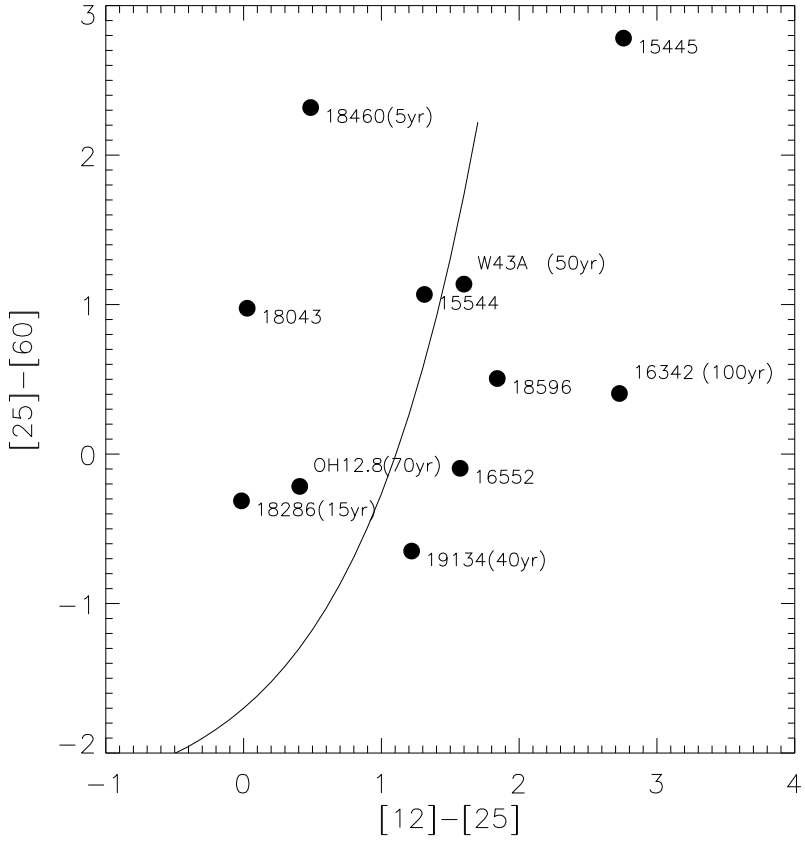

Fig. 3.— Position of the 11 water fountains known up to now in the IRAS two color diagram (see Imai 2007, and references therein). The dynamical age is shown between parentheses for those objects for which it has been calculated. The curve in the plot is the one defined by Bedijn (1987) where the AGB stars tend to be located.

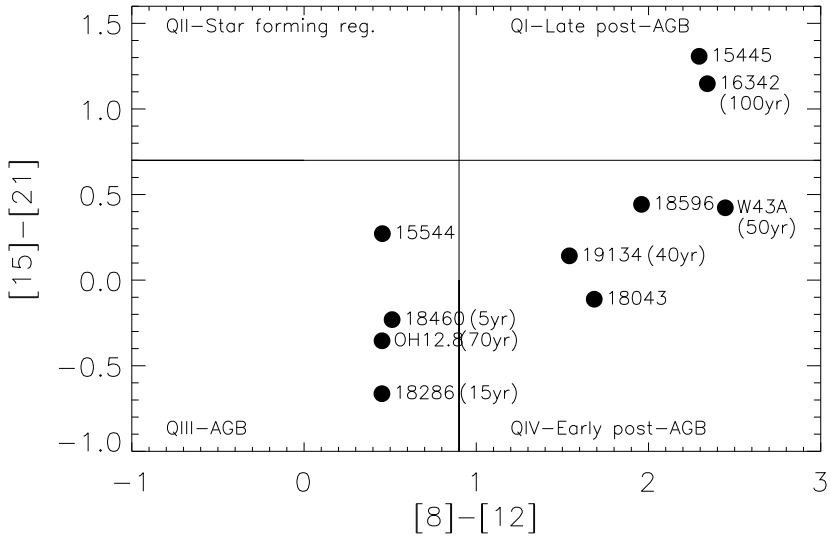

Fig. 4.— MSX two-color diagram of the 10 water fountains known up to now that have been observed with this satellite. The four quadrants are those defined in Sevenster (2002) and described in the text.